

# Comparison of Kinetic Models for Atom Recombination on High-Temperature Reusable Surface Insulation

Ronald J. Willey\*

Northeastern University, Boston, Massachusetts 02115

Five kinetic models are compared for their ability to predict recombination coefficients for oxygen and nitrogen atoms over high-temperature reusable surface insulation (HRSI). Four of the models are derived using Rideal-Eley or Langmuir-Hinshelwood catalytic mechanisms to describe the reaction sequence. The fifth model is an empirical expression that offers certain features unattainable through mechanistic description. The results showed that a four-parameter model, with temperature as the only variable, works best with data currently available. The model describes recombination coefficients for oxygen and nitrogen atoms for temperatures from 300 to 1800 K. Kinetic models, with atom concentrations, demonstrate the influence of atom concentration on recombination coefficients. These models can be used for the prediction of heating rates due to catalytic recombination during re-entry or aerobraking maneuvers. The work further demonstrates a requirement for more recombination experiments in the temperature ranges of 300–1000 K, and 1500–1850 K, with deliberate concentration variation to verify model requirements.

## Nomenclature

$A_N$	= area normal to flux of atoms, $m^2$
$C_a$	= concentration of surface sites for $\delta$ , sites/ $m^2$
$E_a$	= activation energy for adsorption/desorption equilibrium, J/atom or kJ/mole
$E_a$	= activation energy, J/atom or kJ/mole
$h$	= Planck's constant, $6.6256 \times 10^{-34}$ N-m s
$K$	= equilibrium constant for adsorption-desorption, $m^3/\text{atom}$
$K_a$	= pre-exponential coefficient for $K$ , $m^3/\text{atom}$
$k_B$	= Boltzmann constant, $1.38 \times 10^{-23}$ N-m/K atom
$k_i$	= rate constant for reaction step $i$ composed of a pre-exponential coefficient, $k_0$ , and an activation energy, $E_a$
$m$	= mass of an atom, kg/atom
$N_0$	= surface impingement rate of oxygen atoms as given by kinetic theory atoms/ $m^2$ s, $[O][k_B T/2m\pi]^{1/2}$
$[O]$	= concentration of oxygen atoms, atoms/ $m^3$
$[OS]$	= concentration of adsorbed oxygen atoms, atoms/ $m^2$
$P$	= steric factor in Eq. (26), $P_0 \exp(P_2 T)$
$P_i$	= partial pressure of gas species $i$ , Pa
$R$	= universal gas constant, $0.008314$ kJ/mole/K
$[S]$	= concentration of reduced sites on the surface, atoms/ $m^2$
$S_0$	= sticking coefficient in Eq. (26), $S_{01} \exp(S_1 T)$
$[S_0]$	= concentration of total sites on the surface, atoms/ $m^2$
$T$	= temperature at the surface, K
$t$	= time, s
$\delta$	= thermal desorption coefficient, $C_a(k_B T/h) \exp(-D/RT)$
$\gamma_i$	= gamma, recombination coefficient

## Introduction

ATOM recombination is of importance in aerovehicle re-entry. For example, surface temperature-time patterns for space shuttle re-entry can be influenced by the presence of a catalytic surface that promotes atom recombination.<sup>1,2</sup>

At a catalytic surface, the heat flux can double and local surface temperatures can increase 110 K.<sup>1</sup>

The surface temperature increases at a catalytic site because of the accommodation of energy released when two atoms recombine to form molecules. The primary recombination reactions are recombination of O atoms to O<sub>2</sub> (498 kJ released per mole of O<sub>2</sub> formed) and recombination of N atoms to N<sub>2</sub> (945 kJ released per mole of N<sub>2</sub> formed).

The source of O and N atoms are as follows. As a space vehicle re-enters the atmosphere, a bow shock is established off the front nose of the vehicle. As flow goes across the bow shock, molecules are dissociated into atoms. These atoms can then strike the surface of the vehicle, some of which will catalytically recombine back to molecules and leave behind energy that must be dissipated into the surroundings. This paper focuses on the derivation of kinetic equations to describe the recombination rates of atoms on re-entry vehicle surfaces. Specifically, recombination coefficients are modeled as a function of temperature and atom concentration, for recombination on high temperature reusable surface insulation (HRSI) or space shuttle tiles. Space shuttle tiles are composed of about 1–4-in.-thick low-density silica coated with about 3-mm-thick reaction cured glass (RCG). RCG coating is an excellent noncatalytic surface and is ideal for the purpose of low recombination. However, some recombination occurs and must be accounted for in heat shield calculations.

## Background

Recombination coefficients treated in this paper are energy transfer catalytic recombination coefficients for nitrogen and oxygen as defined in Scott.<sup>3</sup> In general, the recombination coefficient  $\gamma$ , is described by an Arrhenius expression

$$\gamma = k_0 \exp(-E_a/RT) \quad (1)$$

where  $k_0$  is called the pre-exponential coefficient and  $E_a$  is called the activation energy.

The Arrhenius expression predicts a nonlinear rise in the recombination coefficient as temperature increases. No maximum appears as temperature is increased, nor is any influence due to the concentration of atoms at the surface described.

In practice, many catalytic reactions do not exhibit constant  $E_a$  over a full range of temperatures of interest. For example, Newman<sup>4</sup> collected data for the recombination of nitrogen atoms on silica. At low temperatures (about 350 K) a rather low activation energy of 4 kJ/mole was shown. As temperature

Received Dec. 6, 1990; revision received Sept. 30, 1991; accepted for publication Nov. 21, 1991. Copyright © 1991 by the American Institute of Aeronautics and Astronautics, Inc. All rights reserved.

\*Associate Professor, Department of Chemical Engineering.

increased from 1000 to 1400 K, the activation energy increased markedly to 100 kJ/mole. Above 1400 K the activation energy decreased markedly, so that above 1600 K, the activation energy became quite negative (about  $-240$  kJ/mole). The reason activation energy varies over temperature is that different reaction steps in the reaction mechanism dominate at different temperatures. For example, at high temperatures, desorption of atoms from the surface is fast, and the apparent activation energy can be negative. This is because equilibrium shifts from adsorption to desorption of atoms from the surface and, therefore, atoms do not stay on the surface long enough to react. Presented below, is data for recombination of atoms on RCG-coated HRSI surfaces which exhibit variable activation energy as a function of temperature. Thus, this work examines two catalytic mechanisms to detect whether kinetic models may be derived that describe the available data. In particular, a maximum in recombination coefficient as a function of temperature appears to exist. Can a mechanistic model describe this maximum?

#### Recombination Data Background

Recombination coefficients for atoms on RCG-coated HRSI surfaces were used in this kinetic model study. The data came from the following sources: Kolodziej and Stewart,<sup>5</sup> Scott,<sup>3</sup> Stewart et al.,<sup>2</sup> (oxygen data only), Willey,<sup>6</sup> Marinelli and Campbell,<sup>7</sup> and Marinelli.<sup>8</sup> Kolodziej and Stewart,<sup>5</sup> Scott,<sup>3</sup> Stewart et al.,<sup>2</sup> and Willey<sup>6</sup> acquired their data from arc plasma test facilities. In arc plasma test facilities, recombination coefficients were determined from the relative heating rates of a known catalytic body compared to the surface being studied. Relations developed by Goulard<sup>9</sup> and later modified by Scott<sup>3</sup> were then used to estimate the recombination coefficient. The work of Marinelli<sup>7,8</sup> was undertaken in a discharge flow reactor. In this work, Marinelli used the ratio of atom concentrations before and after the surface to determine the recombination coefficient.

The recombination coefficient data used in this work is listed in Tables 1 and 2. The first column represents the source of the data. The second column in Tables 1 and 2 presents

**Table 1** Data used in the estimation of parameters for various kinetic models for the recombination of nitrogen atoms on RCG-coated HRSI surfaces

Source	K	[N] <sup>a</sup>	$\gamma_N$
Kolodziej and Stewart <sup>5</sup>	1889	795	0.00894
	1742	862	0.00943
	1686	261	0.01380
	1603	275	0.01465
	1467	300	0.01194
	1422	310	0.01068
	1668	439	0.01945
	1661	366	0.01478
	1582	330	0.01740
	1546	352	0.01499
Scott <sup>3</sup>	1438	232	0.02155
	1387	272	0.01534
	1092	113	0.00943
	1022	91	0.00810
	1014	86	0.00772
	996	67	0.00687
	1536	137	0.01504
	1524	140	0.01401
	1506	134	0.01267
	1496	124	0.01723
Willey <sup>6</sup>	1493	130	0.01464
	1490	129	0.01527
	1460	119	0.01156
	1412	105	0.01383
	1411	107	0.01437
	1402	93	0.01368
	1350	111	0.01540
	300	321	0.00019
Marinelli <sup>7</sup>	300	321	0.00019

<sup>a</sup>[N] atom concentration  $\times 10^{-20}$  in atoms/m<sup>3</sup>.

**Table 2** Data used in the estimation of parameters for various kinetic models for the recombination of oxygen atoms on RCG-coated HRSI surfaces

Source	K	[O] <sup>a</sup>	$\gamma_O$
Kolodziej and Stewart <sup>5</sup>	1831	326	0.00370
	1806	165	0.01007
	1742	171	0.01893
	1726	346	0.00525
	1644	104	0.01068
	1617	185	0.00968
	1592	107	0.03060
	1450	117	0.01790
	1647	163	0.02361
	1493	179	0.01300
Scott <sup>3</sup>	1419	179	0.00775
	1556	210	0.01733
	1344	219	0.01120
Stewart et al. <sup>2</sup>	1557	112	0.00887
	1552	63	0.02793
Willey <sup>6</sup>	1540	119	0.00885
	1527	120	0.01081
	1522	60	0.01637
	1518	115	0.00817
	1501	114	0.01524
	1497	116	0.00838
	1486	112	0.02148
	1479	63	0.01972
	1458	112	0.02432
	1456	62	0.01146
Marinelli <sup>8</sup>	1449	116	0.01500
	300	321	0.00020

<sup>a</sup>[O] atom concentration  $\times 10^{-20}$  in atoms/m<sup>3</sup>.

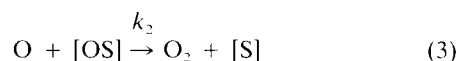
the temperature as read from the figures in the paper, or reported. The third column reports the estimated atom concentration [O], at the surface of the RCG coated test article (for the recombination of nitrogen atoms, substitute nitrogen atom concentration for oxygen atom concentration). Atom concentration was estimated by using the total stagnation pressure times, the estimated atomic mole fraction divided by the Boltzmann constant and temperature (ideal gas law). The fourth column lists the recombination coefficient (gamma) reported or measured.

The data show the general trend of reaching a maximum at about 1600 K. This maximum is not predicted by means of an Arrhenius expression. Thus, kinetic models are developed below that can predict a maximum.

#### Development of Kinetic Models from Reaction Mechanisms

##### Recombination Models Derived from the Rideal-Eley Mechanism

The Rideal-Eley mechanism is a two-step mechanism. First, an atom adsorbs onto a surface site, then the adsorbed surface atom reacts at the surface with a gas phase atom. The mechanism is as follows:



In the first step [Eq. (2)], oxygen atoms are adsorbed onto "reduced" sites. In the second step [Eq. (3)], oxygen atoms near the surface combine with oxygen atoms on the surface to form O<sub>2</sub>, and to regenerate a reduced site. Several kinetic models can be derived from this mechanism. Beginning with the law of mass action, the rate of O<sub>2</sub> production per unit area A<sub>N</sub> is proportional to the concentration of oxygen in the

gas phase times the concentration of oxide sites

$$\frac{dO_2}{A_N dt} = k_2[O][OS] \quad (4)$$

where  $[O]$  is in atoms/m<sup>3</sup> and  $k_2$  has the units m<sup>3</sup>/s atom. At steady state the rate of surface oxide  $[OS]$  site formation has to equal zero

$$\frac{d[OS]}{A_N dt} = 0 = k_1[O][S] - k_{-1}[OS] - k_2[O][OS] \quad (5)$$

If the number of total surface sites is constant then

$$[S_0] = [S] + [OS] \quad (6)$$

or

$$[S] = [S_0] - [OS] \quad (7)$$

Substitution of Eq. (7) into Eq. (5) and solving for  $[OS]$  leads to the following equation:

$$[OS] = \frac{k_1[O][S_0]}{k_1[O] + k_{-1} + k_2[O]} \quad (8)$$

Substitution of Eq. (8) into Eq. (4) leads to

$$\frac{dO_2}{A_N dt} = \frac{k_1 k_2 [O]^2 [S_0]}{k_1 [O] + k_{-1} + k_2 [O]} \quad (9)$$

The recombination coefficient  $\gamma_0$ , is defined as the rate of the number of atoms reacting on the surface per unit area  $dO/A_N dt$ , divided by the number of atoms which strike the surface per unit area-time  $N_0$  or

$$\gamma_0 = \frac{-dO/dt}{A_N N_0} \quad (10)$$

By reaction stoichiometry, the rate of oxygen atom depletion is equal to two times the rate of molecular oxygen formation or

$$\frac{dO}{dt} = \frac{-2 dO_2}{dt} \quad (11)$$

Thus, by the substitution of Eq. (9) into Eq. (11), followed by the substitution for  $dO/dt$  from Eq. (10), and using the definition given by kinetic theory for  $N_0$  with  $N_0 = [O][k_B T/2m\pi]^{1/2}$ , the following expression results for  $\gamma_0$ :

$$\gamma_0 = \frac{2k_1 k_2 [O][S_0][2m\pi/k_B T]^{1/2}}{k_1 [O] + k_{-1} + k_2 [O]} \quad (12)$$

#### Simplification of Eq. (12)

Often the temperature term  $[2m\pi/k_B T]^{1/2}$  is assumed approximately constant in the temperature range of interest, as compared to the exponential terms that exist in the rate constant,  $k_i$ . Thus, the term is combined with a pre-exponential coefficient of the rate constant. Also, if the rate of reaction given in Eq. (3) is rate limiting,  $k_2[O]$  is much smaller compared to  $k_{-1}$  and  $k_1[O]$  in the denominator of Eq. (12). Thus,  $k_2[O]$  can be eliminated from Eq. (12). Dividing top and bottom of Eq. (12) by  $k_{-1}$ , one gets the classical Rideal-Eley mechanism with Eq. (3) as the rate limiting step

$$\gamma_0 = \frac{2k_2 K [O]}{1 + K [O]} \quad (13)$$

$K$  is the equilibrium constant for the adsorption of O atoms onto a reduced surface as given in Eq. (2). Another assumption is that oxygen atom concentration is approximately constant near the surface, and oxygen atom concentration can

therefore, be combined with the pre-exponential coefficients of the rate constant. Thus the result is

$$\gamma_0 = \frac{2k_2 K}{1 + K} \quad (14)$$

Eq. (14) is the simplest four parameter recombination coefficient equation possible. The equation is a function of temperature only with

$$k_2 = k_{20} \exp(-Ea/RT) \quad (15)$$

A similar expression describes the equilibrium constant  $K$

$$K = Ka \exp(D/RT) \quad (16)$$

Where  $Ka$  is the pre-exponential coefficient for the equilibrium constant, and  $D$  is the activation energy related to the adsorption-desorption equilibrium. Equation (14) will be referred to as model 1. When compared to Eq. (1), Eq. (14) has an added term related to adsorption  $[K/(1 + K)]$ . This model predicts that at low temperatures, where adsorption dominates,  $\gamma_0$  will be zero order in oxygen atom concentration in which Eq. (14) reduces to

$$\gamma_0 = 2k_2 \quad (17)$$

At high temperature, the surface will essentially be bare because as temperature increases, fewer oxygen atoms will stay on the surface. Then, the reaction rate can be approximated by

$$\gamma_0 = 2k_2 K \quad (18)$$

The overall results observed are dependent upon the value of  $D$ . The combined  $k_2 K$  term, can have either a positive or negative overall activation energy (called the apparent activation energy). If  $Ea < D$ , then the sum  $(-Ea + D)$  is positive (negative apparent activation energy), and the recombination coefficient will decrease as temperature increases. If  $Ea > D$ , then the sum  $(-Ea + D)$  is negative (positive apparent activation energy) and the recombination coefficient will continue to increase as temperature increases, but at a lower rate than that given by Eq. (17).

Model 1 assumes that the concentration of oxygen atoms near the surface is constant for all conditions. Equation (13) includes the concentration of oxygen atoms at the surface and will be labeled model 2. Model 2, Eq. (13), shows that oxygen atom concentration will influence the recombination coefficient. At low temperatures, model 2 reduces to

$$\gamma_0 = 2k_2 \quad (19)$$

and at high temperatures, model 2 reduces to

$$\gamma_0 = 2k_2 K [O] \quad (20)$$

Therefore, the recombination coefficient reaction order in oxygen concentration will be zero order at low temperatures, and changes to first order at high temperatures. Model 2 shows how recombination coefficients can be a function of atom concentrations near the surface. This paper will demonstrate that there is, unfortunately, not enough data currently available to determine the true functionality of recombination coefficients with surface concentrations.

#### Recombination Coefficient Model Derived from the Langmuir-Hinshelwood Mechanism

In the Langmuir-Hinshelwood mechanism, oxygen atoms adsorb onto the surface to form a surface oxide species. Two neighboring surface oxide species then combine to form mo-

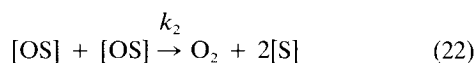
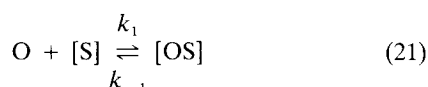
**Table 3 Summary of kinetic models evaluated for the recombination coefficient of N and O atoms on RCG-coated HRSI materials**

Model number	Name	Model
1	Rideal-Eley (no conc. term.)	$\gamma_0 = 2k_2K/(1 + K)$
2	Rideal-Eley	$\gamma_0 = 2k_2K[O]/(1 + K[O])$
4	Langmuir-Hinshelwood	$\gamma_0 = 2k_2(2m\pi/k_B T)^{1/2}K^2[O]/(1 + K[O])^2$
5	Seward	$\gamma_0 = 2PN_0So \exp(-Ea/RT)/[SoN_0 + \delta + PN_0 \exp(-Ea/RT)]$
6	Empirical	$\gamma_0 = 2K(k_2 + k_3)/(1 + K)$

Notes:

 $k_2$  is a function of temperature given by:  $k_2 = k_{20} \exp(-Ea_2/RT)$ . $k_3$  is a function of temperature given by:  $k_3 = k_{30} \exp(-Ea_3/RT)$ . $K$  is a function of temperature given by:  $K = Ka \exp(D/RT)$ . $\delta = C_\delta(k_B T/h) \exp(-D/RT)$ . $P = P_0 \exp(P_2 T)$ . $N_0 = [O](k_B T/2m\pi)^{1/2}$ . $So = S_{01} \exp(S_1 T)$ .[O] is the concentration of oxygen atoms at the surface in atoms/m<sup>2</sup>; for nitrogen atoms substitute [N] for [O] in any of the above models.The value of  $R$  in these models is 0.0083144 kJ/mole/K.

molecular oxygen



Equation (21) represents the adsorption of oxygen onto the surface and is similar to Eq. (2) in the Rideal-Eley mechanism. Equation (22) represents the reaction of two surface oxide species to form molecular oxygen. The resultant recombination model, model 4, is based on the assumption that Eq. (21) is in pseudo-equilibrium and that Eq. (22) is the rate limiting step. Derivation is available.<sup>10</sup> (Model 3 is not presented in this paper, it included the addition of a temperature term to model 2.) The result is

$$\gamma_0 = \frac{2k_2(2m\pi/k_B T)^{1/2}K^2[O]}{(1 + K[O])^2} \quad (23)$$

Model 4 demonstrates that at low temperatures, where adsorption dominates, the recombination coefficient is negative first order in oxygen concentration:

$$\gamma_0 = \frac{2k_2(2m\pi/k_B T)^{1/2}}{[O]} \quad (24)$$

At high temperatures, where adsorption is negligible, the recombination coefficient is first order in oxygen:

$$\gamma_0 = 2k_2(2m\pi/k_B T)^{1/2}K^2[O] \quad (25)$$

Thus, as temperature increases, a transition occurs from negative first order, to positive first order, in oxygen atom concentration at the surface. Once again, the rate constant  $k_2$ , and equilibrium constant  $K$ , follow expressions related to temperature as discussed in the Rideal-Eley mechanism.

#### Recombination Coefficient Rate Model Derived from First Principle Kinetics

Seward<sup>11</sup> developed a recombination coefficient rate model in his 1985 thesis (which is based around the Rideal-Eley mechanism) using first principle kinetics to describe the adsorption, desorption, and reaction rate steps separately. This model, labeled model 5, consists of eight parameters:

$$\gamma_0 = \frac{2PN_0So \exp(-Ea/RT)}{SoN_0 + \delta + PN_0 \exp(-Ea/RT)} \quad (26)$$

The term  $P$  represents the steric factor and is related to the ability of oxygen atoms to adsorb. Seward allowed this factor to be a function of temperature up to a certain constant. (See the notes below Table 3 for the mathematical expression of  $P$  as a function of temperature.) The  $So$  term is related to the sticking coefficient, and predicts the probability that an atom will adhere, once it strikes the surface. Seward allowed for this to be a function of temperature. The exponential term in the numerator, is related to the forward reaction rate of step 2, Eq. (3), in the Rideal-Eley mechanism. The term  $\delta$  in Seward's equation, is related to the desorption step in Eq. (2) of the Rideal-Eley mechanism, and consists of an activation energy and a constant related to the number of surface sites. Model 5 has three characteristic temperature ranges. At low temperatures, adsorption of atoms onto the surface  $SoN_0$ , dominates, and model 5 reduces to

$$\gamma_0 = 2P \exp(-Ea/RT) \quad (27)$$

As temperature increases, the forward reaction rate of Eq. (3) increases. Thus, the exponential term,  $PN_0 \exp(-Ea/RT)$ , dominates in the denominator and the numerator, and  $\gamma_0$  is given by

$$\gamma_0 = 2So \quad (28)$$

At high temperatures, the desorption of oxygen atoms  $\delta$ , dominates and the following approximation results:

$$\gamma_0 = [2PN_0So \exp(-Ea/RT)/\delta] \quad (29)$$

Model 5 predicts zero reaction order at low and medium temperatures in oxygen atom concentration; at higher temperatures, the model becomes first order in oxygen atom concentrations. The steric factor and the sticking coefficient in model 5 are allowed to be a function of temperatures. An attractive feature of this model, is that it predicts low activation energy for recombination at low temperatures, changing to a higher activation energy at moderate temperatures. The difficulty in the application of model 5, is the determination of the eight parameters due to too many parameters for the currently available data.

#### Empirical Model for Recombination Coefficient

A six parameter empirical model, model 6, is compared to the data available

$$\gamma_0 = \frac{2(k_2 + k_3)K}{1 + K} \quad (30)$$

This model can be thought of as the combination of two mechanistic steps, the rate being determined by the fastest of the two steps, with each step dependent upon an activation energy. In this work, the rate constant  $k_3$  dominates at low temperatures. The recombination coefficient is described by  $k_3$  at moderate temperatures and it is described by  $2k_2K$  at high temperatures.

Using the proper parameters, model 6 has a low apparent activation energy at low temperatures. Further, as temperature increases, the apparent activation energy increases. Finally, at high temperatures (where desorption dominates), the overall activation energy goes from positive to negative and, therefore, the recombination coefficient declines as temperature further increases. Information concerning concentration dependence of recombination coefficients is lacking. Therefore, a concentration term is not included in model 6. A summary of mechanistic models evaluated in this article is shown in Table 3.

#### Determination of Constants

For the models presented above, the parameters were determined by nonlinear least squares fit on the log of the recombination coefficient  $\gamma$ . The log of  $\gamma$  was chosen because it would give equal weight to lower  $\gamma$  at lower temperatures. Therefore, the parameters chosen, were those which minimized the sum of squares of error (SSE) defined as

$$\text{SSE} = \sum [\log(\gamma_{(i)\text{obs}}) - \log(\gamma_{(i)\text{pred}})]^2 \quad (31)$$

All plots presented are  $\log \gamma_i$  vs  $1/T$ . The parameters for models 1–4 were determined by using a nonlinear least squares routine, BMDP PAR,<sup>12</sup> for derivative-free nonlinear models. To provide assistance in determination of constants by nonlinear least squares, the models were reparameterized as suggested in Draper and Smith.<sup>13</sup> This resulted in faster converging least squares routines. A limit was also placed on the maximum value of  $D$ , the desorption activation energy, of 574 kJ/mole, preventing arithmetic overflows during the determination of the constants.

The constants for model 5 were determined using LOTUS 123,<sup>14</sup> with a single parameter perturbation interactive approach. Each parameter was individually varied to determine the direction of the sum of SSE on  $\log \gamma$ . Then, depending upon which parameter reduced the SSE the most, that parameter was corrected and new parameters were found. The parameters for model 6 were determined by choosing activation energy for the low-temperature reaction coefficient,  $k_3$ . The values used were 2.67 kJ/mole for nitrogen, and 4.19 kJ/mole for oxygen atoms. These values were used for the recombination of atoms on silica at low temperature in Newman's<sup>4</sup> and Seward's<sup>11</sup> theses. The remaining parameters in that model were determined by nonlinear least squares.

#### Application of the Models

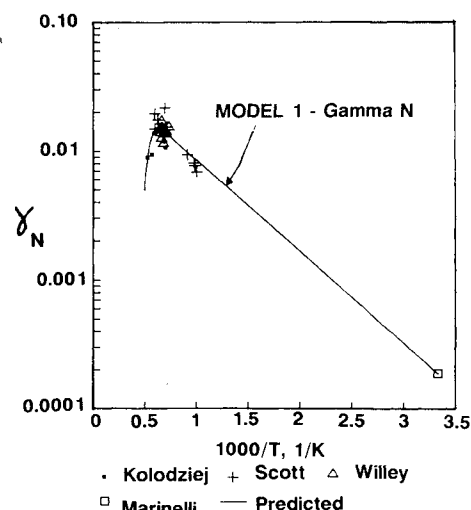
Table 4 presents the overall summary for the residual sum of squares achieved by regression. The models are compared for their ability to predict recombination data for the recombination of nitrogen and oxygen atoms on RCG-coated HRSI materials. The best fits were achieved by model 1, as demonstrated by the low SSE in Table 4 for both cases. Model 6 also closely resembles the data, giving a slightly lower SSE for nitrogen and slightly higher SSE for oxygen. Figure 1 illustrates model 1 for the recombination of nitrogen atoms on RCG coated HRSI surfaces.

Figure 1 shows a maximum in recombination coefficient as temperature increases. The maximum occurs at about 1600 K, with a maximum predicted recombination coefficient of 0.013 for nitrogen and 0.014 for oxygen. Residual plots (not shown) confirm the suitability of this model. The only trend that appears is for residuals plotted as a function of concentration. The trend is slightly negative, indicating that the model is slightly deficient in concentration terms.

**Table 4** Residual sum of squares summary for various recombination coefficient models

Model number	Name	SSE <sup>a</sup> for nitrogen	SSE for oxygen
1	Arrhenius	0.254	1.357
	Rideal-Eley without concentration terms	0.138	0.938
2	Rideal-Eley	0.150	1.044
4	Langmuir-Hinshelwood	2.259	1.019
5	Seward's	0.206	1.134
6	Empirical	0.136	1.021

<sup>a</sup>Sum of squares of errors on  $\log \gamma$ .



**Fig. 1** Comparison of model 1 with data for the recombination coefficient for nitrogen atoms on RCG-coated HRSI material.

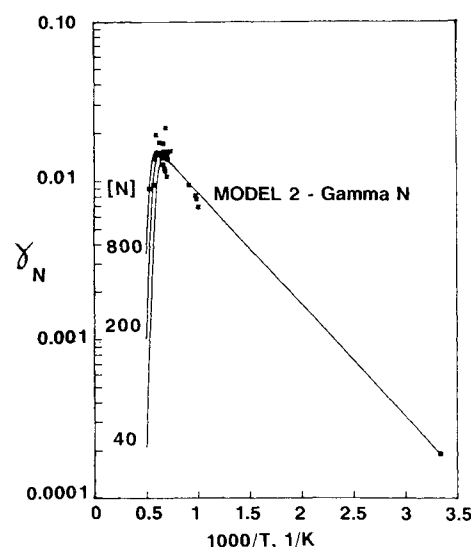


**Fig. 2** Comparison of model 2 with data for the recombination coefficient for nitrogen atoms on RCG-coated HRSI material.  $[N]$  is  $10^{20}$  atoms/m<sup>3</sup>.

Example of the results predicted by model 2 are shown for the nitrogen atom recombination coefficient in Fig. 2. The recombination coefficient has a first-order functionality in concentration at higher temperatures (left side of Fig. 2). At low temperatures, the three concentration predictions combine into a single curve on the right side of Fig. 2, because the concentration functionality is zero order. The model predicts a maximum in recombination as a function of temperature, and it also predicts a concentration dependence at higher

temperatures. The plot for model 2 of oxygen atom recombination is very similar to that of nitrogen shown in Fig. 2.

The residual plots for model 2 had wider residuals compared with model 1, and showed negative trends for oxygen and nitrogen atom concentrations. These residual plots (as a function of concentration) indicate that the model should be at least one order less in concentration.

The addition of a temperature concentration term to model 2 ( $2m\pi/k_B T$ )<sup>1/2</sup> did not enhance the fit of data (this was labeled model 3 that is not presented in this article). A slight concave downward appearance occurs in the curves for the low temperature region between 300–1000 K on  $\gamma_i$  vs  $1/T$  plots. This appearance occurs because of the  $T^{1/2}$  in the numerator.

Model 4, the Langmuir-Hinshelwood model, showed a very poor fit for the nitrogen data and a good fit for the oxygen data, shown in Fig. 3. In determining the parameters for nitrogen atom recombination in Model 4, boundaries were reached in which an arithmetic overflow occurred during the computational steps. Therefore, the parameters chosen are at the boundary for  $Ka$  and for  $D$ . The model essentially looks like a negative first-order for nitrogen atoms throughout the whole region. In Fig. 3, the recombination rate is higher for lower partial pressures for oxygen atoms with the curves at 100, 400, and 800 Pa, falling beneath each other sequentially. (Atom concentration is related to the partial pressure by the ideal gas law relation,  $[O] = P_O/k_B T$ .) The data (which had different pressures depending upon the researcher) were well described by model 4, considering the wide range of variables studied. The Langmuir-Hinshelwood model explains the observation of higher recombination rates at lower oxygen atom concentrations. Because the reaction requires two neighboring sites, a maximum in the recombination coefficient is reached in this model as a function of concentration. This maximum occurs when the surface is about half-covered with adsorbed atoms; when half of the sites are empty, and half of the sites are covered. When the surface is base no reaction occurs, because nothing is on the surface. At the other extreme, when the surface is covered at higher atom concentrations, atoms that are near the surface cannot adsorb until two atoms combine on the surface and desorb, therefore, the maximum occurs when the surface is half-covered. Although good data is unavailable to confirm this model, experiments need to be conducted at temperature regions between 500–1000 K with the concentration of oxygen atoms purposely varied, in order to determine an influence of recombination coefficient as a function of concentration.

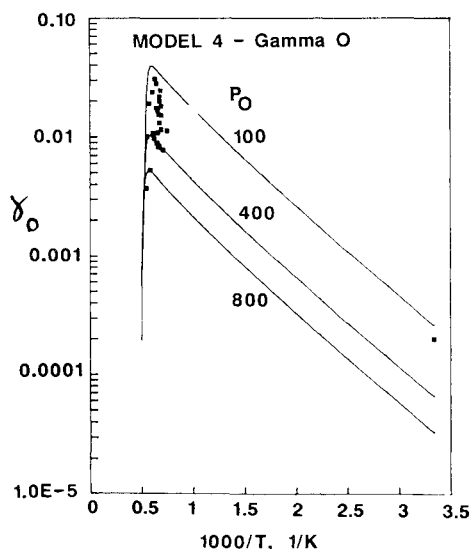


Fig. 3 Comparison of model 4 with data for the recombination coefficient for oxygen atoms on RCG-coated HRSI material.  $P_O$  is in Pa,  $[O] = P_O/k_B T$ .

The results for model 5 are shown in Fig. 4 for the oxygen atom recombination coefficient. In Fig. 4, as the temperature increases, the activation energy increases (going from right to left from  $1/T = 0.0033$  to  $0.001$ , or  $T = 300$  K to  $1000$  K). Seward's model achieves this by changing the parameters  $P$  and  $S$ , and a maximum  $\gamma$  is reached at about  $1600$  K. At temperatures above  $1600$  K,  $\gamma$  decreases and the functionality is first order in the partial pressure of atom concentration. At high temperatures, model 5 is very similar to the Rideal-Eley mechanism. The residual plots for model 5 show good scatter of the data points around zero. Plots for  $\gamma_N$  show similar curves.

Comparison of model 6 to the data is shown in Fig. 5 for oxygen atom recombination coefficients. This particular model has no concentration term, but does predict that the recombination coefficient will increase to a maximum as temperature increases, and then decrease as temperature increases further. Model 6 also demonstrates increasing activation energy as temperature increases in the low temperature region ( $300 < T < 1000$  K). An increasing activation energy (as temperature increases) is based on data from atom recombination on silica type surfaces<sup>1-11</sup> that are very similar to RCG coated surfaces. The apparent activation energy is the com-

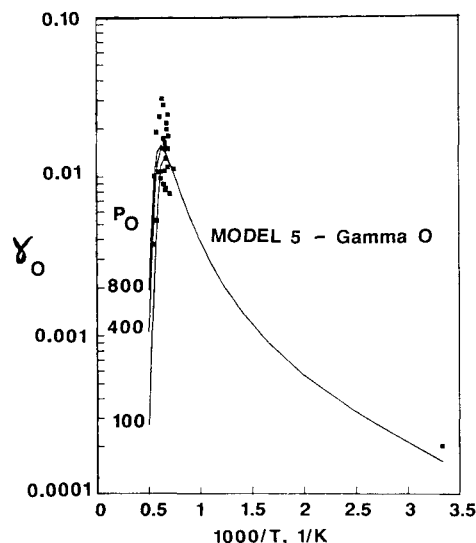


Fig. 4 Comparison of model 5 with data for the recombination coefficient for oxygen atoms on RCG-coated HRSI material.  $P_O$  is in Pa,  $[O] = P_O/k_B T$ .

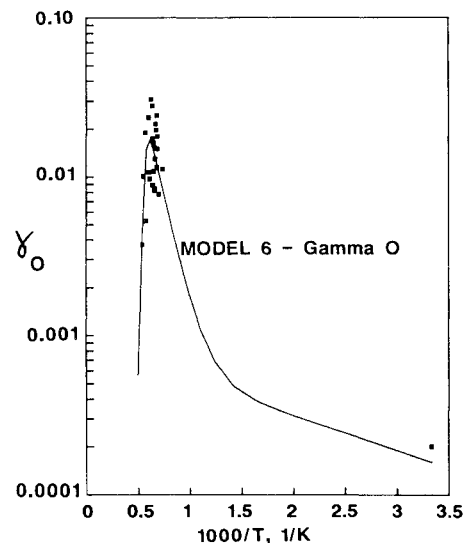


Fig. 5 Comparison of model 6 with data for the recombination coefficient for oxygen atoms on RCG-coated HRSI material.

**Table 5** Parameter estimates for various recombination models evaluated

Model number	Parameter name	Parameter units	Value for N atom recombination	Value for O atom recombination
1	$k_{20}$	unitless	0.021953	0.020155
	$Ea_2$	kJ/mole	13.580	13.235
	$Ka$	Unitless	1.0647E-07	5.7376E-16
	$D$	kJ/mole	249.318	520.880
2	$k_{20}$	unitless	0.021660	0.019763
	$Ea_2$	kJ/mole	13.545	13.186
	$Ka$	m <sup>3</sup> /atom	1.2309E-33	8.6919E-40
	$D$	kJ/mole	359.890	574.340
4	$k_{20}$	atoms/m <sup>2</sup> /sec	1.5283E + 23	8.1484E + 22
	$Ea_2$	kJ/mole	14.209	12.676
	$Ka$	m <sup>3</sup> /atom	1.9649E-19	1.8112E-38
	$D$	kJ/mole	574.340	574.340
5	$D$	kJ/mole	353.500	339.000
	$Ea$	kJ/mole	4.593	4.185
	$C_a$	atoms/m <sup>2</sup>	1.10E + 20	7.94E + 19
	$P_0$	unitless	2.25E-04	1.79E-04
	$P_2$	1/K	3.12E-03	2.92E-03
	Max $P$	unitless	0.04	0.10
	$S_{01}$	unitless	3.16E-01	5.01E-01
	$S_1$	1/K	-2.00E-03	-2.00E-03
6	$k_{20}$	unitless	3.9885E-02	7.4805E-01
	$Ea_2$	kJ/mole	20.409	58.861
	$k_{30}$	unitless	2.4275E-04	4.2845E-04
	$Ea_3$	kJ/mole	2.677	4.189
	$Ka$	unitless	2.8098E-08	1.4158E-14
	$D$	kJ/mole	262.921	458.036

See Table 3 for the definition of each model.

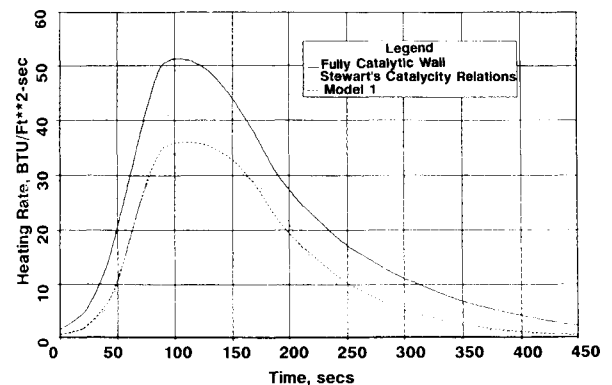
bination of two parallel reaction's activation energies, one reaction going faster at low temperatures and the other speeding up at high temperatures. The activation energy chosen for the low temperature reaction was based on values reported by Newman (1987)<sup>4</sup> and Seward (1985)<sup>11</sup> for nitrogen and oxygen atoms, respectively. They reported the activation energy to be 2.67 kJ/mole for nitrogen atom recombination, and 4.17 kJ/mole for oxygen atom recombination on silica surfaces at low temperatures. The residual plots for model 6 demonstrated a good fit in all cases, with the exception of a slight negative trend in terms of the pressure for oxygen.

Table 5 presents the parameter estimates for the various recombination models evaluated. Column 1 represents the model number that corresponds to the model presented in Table 3; columns 2 and 3 present the parameter name and its units. Rate constants and equilibrium constants are composed of two terms, a pre-exponential coefficient and an activation energy. Columns 4 and 5 are the parameter values which give the minimum SSE for the comparison of each model to the data. The confidence limits for the parameters are not presented because of the poorly conditioned nonlinear surfaces encountered with these models.

In summary, a model independent of concentration describes the available data. The recombination model can be one of two versions, depending upon future results of low temperature recombination experiments. If data falls in the lower regions at 500 K, model 6 should be used, if data falls upon a straight line between 300–1000 K, model 1 is more appropriate. If, in further work, a concentration functionality is found important, then data should be compared to models 2, 4, and 5 (Figs. 2–4).

#### Application of Model 1 to Heating Rate Determination for the Aeroassist Flight Experiment

The application of model 1 to predict heating rates as a function of time for a re-entry trajectory of the aeroassist flight experiment was computed by Mr. Stan Bouslog of Lockheed Engineering and Sciences Company. Figure 6 compares the predicted heating rates of Kolodziej and Stewart's catalytic models, that are discontinuous as a function of tem-



**Fig. 6** Comparison of stagnation point convective heating rates predicted by using the expressions for  $\gamma$  given by model 1 to a fully catalytic wall and Kolodziej and Stewart's catalytic expressions.

perature, to model 1 that is a continuous model in temperature. Model 1 predicts slightly higher heating rates early in the re-entry pattern, compared to Kolodziej and Stewart models. However, model 1 predicts much lower heating rates when compared to the fully catalytic wall (shown by the solid curve in the figure). A brief transition occurs where model 1 predicts a lower heating rate than that predicted by Kolodziej and Stewart, because model 1 predicts a lower recombination coefficient in this region. The peak heating rate occurs about 110 s into the re-entry trajectory. The maximum heating rate for model 1 is about 35 Btu/ft<sup>2</sup>/s, compared to the maximum heating rate of about 33 Btu/ft<sup>2</sup>/s predicted by Kolodziej and Stewart catalytic models. Model 6 was also examined in the simulation, and showed results similar to model 1. Thus, the goal of providing design engineers with a continuous recombination model for atom recombination on surfaces has been achieved.

#### Conclusions

Recombination models for oxygen and nitrogen atoms on surfaces can be derived from the Rideal-Eley mechanism,

which describes observed recombination data on RCG-coated HRSI surfaces. The most appropriate model was dependent in temperature only and included an adsorption equilibrium term in the numerator and denominator. Rideal-Eley rate models for recombination coefficients are usually zero order in concentration at low temperatures, and first order at high temperatures; however, available data do not support inclusion of concentration terms into recombination coefficient models. Two recombination models were applied to stagnation point heating rate simulations, and illustrate similar heating rates to those achieved by catalytic relations discontinuous in temperature. Parameter estimation in all of the models is difficult, requiring reparameterization and possible predetermination of some constants.

More experimental work is recommended in two temperature regions, 300–1000 K and 1500–1800 K, regarding atomic recombination rates on RCG-coated HRSI materials. Additional experiments, that vary the concentration (partial pressure) of atoms at the surface, are also necessary. In summary, depending upon the results, one of the four models presented above can be used for the description of recombination coefficients on RCG-coated HRSI materials. If additional experiments support no concentration dependency, then model 1 or 6 should be chosen (model 6 if the apparent activation energy increases in the temperature range from 300 to 1400 K, model 1 if the constant activation energy occurs from 300 to 1400 K). If concentration dependence is found, then model 2 or 4 should be chosen (model 2 if the recombination coefficient is found to be zero order at low temperatures and first order at high temperatures, model 4 if the recombination coefficient is found to be negative first order and makes a transition to first order as temperature increases).

### Acknowledgments

This work was supported by NASA Grant NAG-9-314. The author acknowledges Caryn Vigoda, Department of Chemical Engineering, Northeastern University, for her assistance in editing this manuscript. The author also acknowledges David J. Blake, M.S., Chemical Engineering, Department of Chemical Engineering, 1989, for his assistance in the creation of the data base. The author also appreciates the assistance of Stan Bouslog and the Lockheed Engineering and Sciences Company for the evaluation of reaction models in terms of

the AFE baseline trajectory heating rates. Carl Scott is most gratefully acknowledged for his advice and assistance throughout the project and manuscript preparation.

### References

- <sup>1</sup>Scott, C. D., "Effects of Nonequilibrium and Wall Catalysis on Shuttle Heat Transfer," *Journal of Spacecraft and Rockets*, Vol. 22, No. 5, 1985, pp. 489–499.
- <sup>2</sup>Stewart, D. A., Rakich, J. V., and Lanfranco, M. J., "Catalytic Surface Effects Experiment on the Space Shuttle," *Thermophysics of Atmospheric Entry*, edited by T. E. Horton, Vol. 82, Progress in Astronautics and Aeronautics, AIAA, New York, 1982, pp. 248–272.
- <sup>3</sup>Scott, C. D., "Catalytic Recombination of Nitrogen and Oxygen on High-Temperature Reusable Surface Insulation," *Aerothermodynamics and Planetary Entry*, edited by A. L. Crosbie, Vol. 77, Progress in Astronautics and Aeronautics, 1981, pp. 192–212.
- <sup>4</sup>Newman, M., "A Model for Nitrogen Atom Recombination on a Silicon Dioxide Surface," M.S. Thesis, Air Force Inst. of Technology, AFIT(GE)ENG/87D-50, Wright-Patterson AFB, OH, 1987.
- <sup>5</sup>Kolodziej, P., and Stewart, D. A., "Nitrogen Recombination on High-Temperature Reusable Surface Insulation and the Analysis of its Effects on Surface Catalysis," AIAA Paper 87-1637, June 1987.
- <sup>6</sup>Wiley, R. J., "Arc Jet Diagnostics Tests, Final Report," NASA-JSC/ASEE SFFP, 1988.
- <sup>7</sup>Marinelli, W. J., and Campbell, J. P., "Spacecraft-Metastable Energy Transfer Studies: Final Report," NAS9-17565, July 1986.
- <sup>8</sup>Marinelli, W. J., "Collisional Quenching of Atoms and Molecules on Spacecraft Thermal Protection Surfaces," AIAA Paper 88-2667, June 1988.
- <sup>9</sup>Goulard, R., "On Catalytic Recombination Rates in Hypersonic Stagnation Heat Transfer," *Jet Propulsion*, Vol. 28, Nov. 1958, pp. 737–745.
- <sup>10</sup>Wiley, R. J., "Mechanistic Model for Catalytic Recombination During Aerobraking Maneuvers," NASA CR 185611, 1989.
- <sup>11</sup>Seward, W. A., "A Model for Oxygen Atom Recombination on a Silicon Dioxide Surface," Ph.D. Dissertation, Air Force Inst. of Technology, AFIT/DS/AA/85-1, Wright-Patterson AFB, OH, 1985.
- <sup>12</sup>BMDP *Statistical Software*, edited by W. J. Dixon, Univ. of California Press, Berkeley, CA, 1983.
- <sup>13</sup>Draper, N., and Smith, H., *Applied Regression Analysis*, 2nd ed., Wiley, New York, 1981, p. 488.
- <sup>14</sup>LOTUS 123 *Reference Manual Release 2*, Lotus Development Corp., Cambridge, MA, 1985.